Journal of Structural Geology, Vol. 3, No. 3, pp. 253 to 264, 1981.
Printed in Great Britain

0191-8141/81/030253-12 $02.00/0

The application of computer-assisted photogrammetric methods in the structural analysis of part of the North Greenland Fold Belt

STIG A. SCHACK PEDERSEN

Geologisk Centralinstitut, Øster Voldgade 10, DK-1350 Copenhagen K, Denmark

(*Received* 11 *December* 1980; *accepted in revised form* 27 *April* 1981)

Abstract—The development of computer support in photogrammetric measurements has facilitated quick calculations of structural geological elements such as strike and dip, fold axes and axial planes. Computer-assisted photogrammetric methods have been applied in a structural analysis of 3000 km² in central Peary Land, North Greenland. Detailed studies have been carried out in an area covered by a single stereo model representing part of the southernmost margin of the North Greenland Fold Belt. On the basis of the aerial photos, a map with both lithological boundaries and structural measurements may be drawn. In little known areas with complex structural relationships field work is necessary to control the interpretation. In the present study refolded thrust fault structures were investigated. Preparatory photogrammetric studies allow the limited time available for field work to be effectively utilised, and accurate geological maps to be produced relatively quickly.

INTRODUCTION

IN GEOLOGICAL mapping, aerial photos can be used at various levels of sophistication from simply a supplement to the topographic map, to advanced photogeological interpretation (e.g. Miller 1961, Lattman & Ray 1965). In general only a mirror stereoscope is used with an ordinary manual adjustment of the photos so that they form a stereo model; this is often sufficient for a photogeological interpretation. Most geologists seem to have been discouraged from obtaining exact measurements of geological structures under a mirror stereoscope because of the time involved in making parallax bar measurements of single stereo points. Advanced photogrammetric instruments such as stereo plotters have been applied occasionally for large scale mapping (1:10,000– – 1:50,000), but the cost of these instruments and the time demanded for exact relative and absolute orientation has previously prevented intensive use of these methods. However, since 1975 K. Dueholm has worked on the development of numerical photogrammetric methods, that with the aid of a computer have greatly increased the efficiency of stereo plotters in photogeology (Dueholm 1979).

In the last five years the Geological Survey of Greenland (GGU) has been involved in the development of computer supported photogeology (Dueholm 1976, Dueholm *et al.* 1977, Dawes 1977, Jepsen & Dueholm 1978). In North Greenland, where the application of aerial photos is facilitated by the sparseness of the vegetation, and where climate and inaccessibility impose strong limitations on field work, the application of rapid methods in photogeology became of primary importance, and in 1978 a Kern PG 2 instrument (see later) was purchased for the mapping project.

The aim of this paper is to describe how these photogrammetric methods have been applied in a photogeologically supported structural analysis. The area studied, covering *c.* 3000 km², straddles Frederick E. Hyde Fjord (Fig. 10. For location see Fig. 6). The analysis is part of the structural mapping of a larger part of central Peary Land. One of the stereo models has been selected to demonstrate in detail how the photogrammetric method is used.

On the basis of the photogrammetric mapping supported by a two-month field season it was possible to show that the southern margin of the North Greenland Fold Belt in Peary Land is characterised by refolded thrust fault deformation over an area of at least 2500 km².

METHODS

The instrument applied in this study is the Kern PG 2-D stereo plotter with *x*, *y*, *z* encoders and the digitizing module DC 2-B connected to a Hewlett Packard 9825A desk-top computer installed at GGU, Copenhagen. The instrument data and functions have been described by Dueholm (1979).

The basis for working with the instrument is the continuous computer registration of the position of the *floating mark* (for definition see Wolf 1974) from the stereoscopic model.

In the Kern PG 2 instrument the path followed by the floating mark in the stereo model is drawn by an internal pantograph at the scale of the model. At the same time the coordinates are digitized and transmitted to the HP9825A computer where they can be tape-recorded for later transfer to a graphic plotter and/or be used in calculations of the orientation of geological structures. Jepsen & Dueholm (1978) and Dueholm (1979, 1980) have devised special functions by which geological data such as strike and dip, fold axis, thickness of lithostratigraphical section etc. may be calculated.

In a study of the type described in this paper the working procedure for a model, after it has been orientated in the instrument by an operator, is as follows: First the topography is drawn and recorded; this operation can be partly or wholly carried out by the operator. Then the

geologist takes over entirely and the geological calculations are carried out by means of the special programs. Having completed the geological interpretation and calculations, the geological features such as boundaries, traces of bedding planes, faults and dykes are recorded. After all the work on the stereoscopic model is completed, the data recorded are transmitted to a PDP computer and a plot of the geological–topographical map is drawn on a Calcomp drum plotter.

Production of maps

Generally it is only necessary to draw the topography in areas where no maps are available, as in the area studied and adjacent parts of North Greenland, or where the maps are unsatisfactory. However, little extra work is needed to obtain a comprehensive topographic base map for the geological map. The topography is drawn in two stages: (a) coast lines, ice caps, lakes and streams, (b) contours (100-m intervals). Geological boundaries and other geological features are drawn in the same way as streams and ice caps. The trace of a geological feature across areas covered by ice or younger deposits can be extrapolated using the z-guiding facility described by Dueholm (1979, 1980). The principle for z-guiding is that the z-coordinate of the floating mark is guided by a feedback from the computer to the plotting instrument while x and y coordinates are driven manually. The computer tracing of the floating mark is very similar to the tracing of contour lines in topographic mapping, with the difference that the floating mark is guided to follow an already digitized and calculated inclined geological surface.

Using a code system it is possible to discriminate between topographic lines and geological lines during the retrieval of data for the required map. This permits later production of maps with any of the following combinations: topographic boundaries and geological lines, contours and geological lines, all topographic lines together with geological symbols (strike/dip, fold axes and other symbols), and finally all topographic lines and geological lines and symbols. At present, four types of lines are used, and three colour pens are available. This gives a more readable plot than the plot-map shown in Fig. 5. The computer can compile maps covering two or more models from the stored data at any scale requested.

Calculations of structural elements

The basis for the geological calculations is the determination of the spatial relationships of a geological plane. This may be calculated from at least three points measured in the stereo model by application of the equation.

$$\mathbf{a}x+\mathbf{b}y+\mathbf{c}z+d=0,\ \mathbf{a}^2+\mathbf{b}^2+\mathbf{c}^2=1$$

where (**a**, **b**, **c**) is a normal unit vector to the plane. In general several points (more than 10) are measured and the best fitting plane is calculated by least squares adjustment. The following coefficients in the normal equations for a least squares adjustment are given by:

$$N(0)=n,\ N(1)=\Sigma x,\ N(2)=\Sigma y,\ N(3)=\Sigma z$$
$$N(4)=\Sigma xx,\ N(5)=\Sigma yy,\ N(6)=\Sigma zz$$
$$N(7)=\Sigma yz,\ N(8)=\Sigma xz,\ N(9)=\Sigma xy$$

where n is the number of points. These coefficients can be summed point by point so that only ten registers are used, regardless of the number of points. Therefore the points can be obtained incrementally, without capacity problems, as a geological horizon is traced by the floating mark. This has proved to facilitate the measurements. For a measured and calculated plane the orientation, the standard error on the strike and dip angles and the standard error on the distance from observed points to the plane are given (Dueholm 1979, 1980) (Fig. 1).

The calculation of the orientation of the plane furthermore constitutes the basis for measuring stratigraphical sections. In this procedure a datum plane, which should have a strike and dip representative for the section, is measured first. Then the datum plane is displaced parallel to the base of the section (or to the top if more convenient), and the stratigraphical section can be measured orthogonally to the datum plane.

A geologist working with stereo photographs must always possess a critical sense for spatial geometry when the choice of structures to be measured is made. It should be borne in mind that a measurable plane must be exposed in three dimensions. In many places well exposed strata in steep cliff sections must be discarded because the measured points will represent a straight line due to the absence of exposures in an orthogonal direction. Similarly too little relief impedes reliable measurements.

Fold structures are investigated on the basis of discrete measurable bedding planes across the fold (Fig. 2). In the fold axis calculation the normal vectors to the measured planes are weighted according to their standard error and the extent of the measured area (Dueholm 1979, p. 65) (Fig. 3).

A recurring problem is to decide at which values of

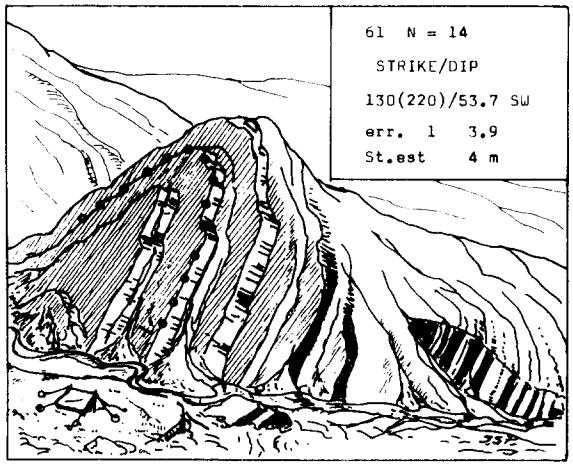

Fig. 1. Illustration to show how the floating mark points (small circles) are placed on the bedding plane of an exposure. The instrument measurement is given in the upper right corner. 61 is the number of the bedding plane measured in the stereo model, 130 is the strike, 220 the direction of dip, 53.7 SW the angle of dip, 1 the standard error on strike, 3.9 the standard error on dip, and St.est. 4 m is the standard error of estimate of distance from point to calculated plane.

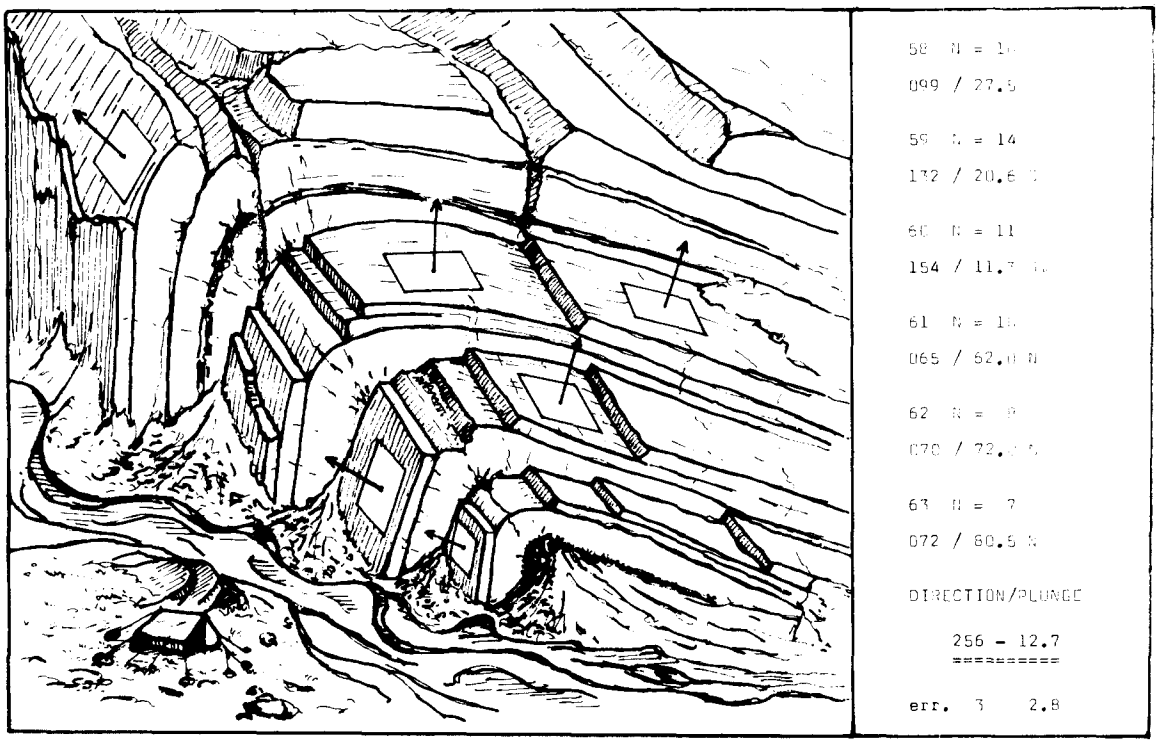

Fig. 2. Strike and dip measurements for fold axis calculation. A number of discrete planes in the fold structure are measured. In the table to the right the number of each bedding plane measured is given, the number of points measured in each strike-and-dip (e.g. $N = 10$), and the strike and dip of each plane (e.g. 099/27.5 S). The fold axis calculation is based on the cross product of the poles to the planes, and the standard error for the direction and plunge is given.

standard error a fold axis calculation must be rejected. This can only be solved through a general knowledge of the structural geology of the area, and the geologist's experience, supported if possible by field investigations. If the standard error seems to be unacceptable the working procedure developed at GGU permits measurement of additional planes. It is a considerable advantage that fold axis calculations can be made immediately after measurement of the planes and the need for additional measurements thus revealed while the stereo model is still in position.

APPLICATION OF THE METHOD IN THE FREDERICK E. HYDE FJORD REGION

The Frederick E. Hyde Fjord region lies in the central part of Peary Land at the southern margin of the North Greenland Fold Belt. The rocks involved in the fold belt in this area are Lower Palaeozoic clastic trough sediments (Dawes & Soper 1973, 1979, Surlyk *et al.* 1980). The subarea of Nordkroneli is situated south of Frederick E. Hyde Fjord and represents the absolute southern limit of

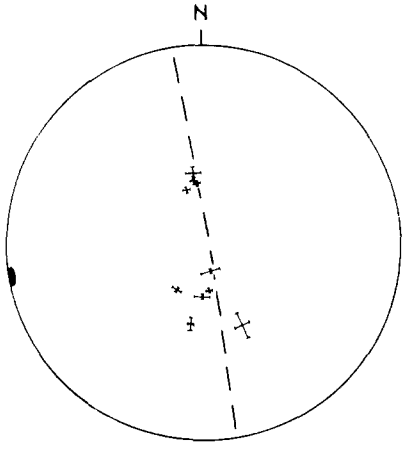

N	STRIKE/DIP		err.	St.est.(m)
21	083/29.5	S	3/2.3	3
19	085/25.3	S	1/0.9	2
21	082/26.3	S	1/1.0	3
21	074/22.7	S	1/1.0	3
16	098/34.2	N	1/2.9	2
16	118/22.1	NE	2/1.3	1
29	073/11.9	N	4/0.5	3
24	090/21.9	N	3/0.9	2
31	065/37.8	NW	3/5.9	4
34	081/19.6	N	1/0.4	3

Fig. 3. Stereogram of the calculated fold axis 261°/2° (for location see Fig. 5), equal area projection, lower hemisphere. The poles to the planes are marked with crosses where the length of the arms equals the standard error. The black area marks the standard error of the fold axis.

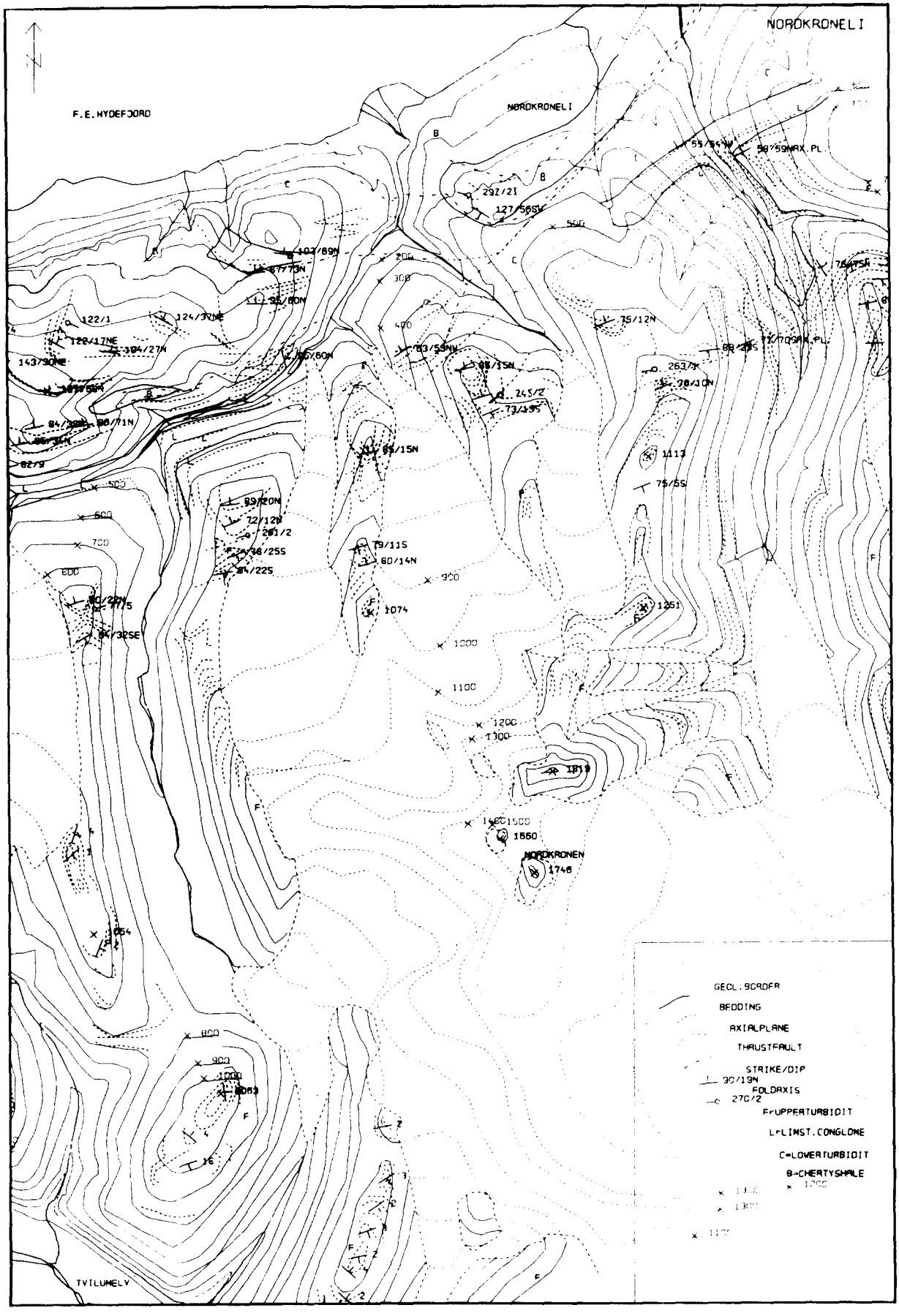

Fig. 5. Calcomp plot of the recorded observations in the stereo model Nordkroneli. The area covers 15 × 21 km. The plot is reproduced exactly as delivered by the plotter with all the limitations this involves. The author thus deliberately refrained from adding to or 'improving' the figure.

Fig. 4. The stereoscopic model Nordkroneli, parts of the arial vertical photos GI 874E 1106 and 1108, scale 1:150,000 (copyright Geodetic Institute, Denmark, published with permission no. A.495/78). Frederick E. Hyde Fjord is seen in the upper part of the model; in the central part the Nordkronen mountain rises towards the eye.

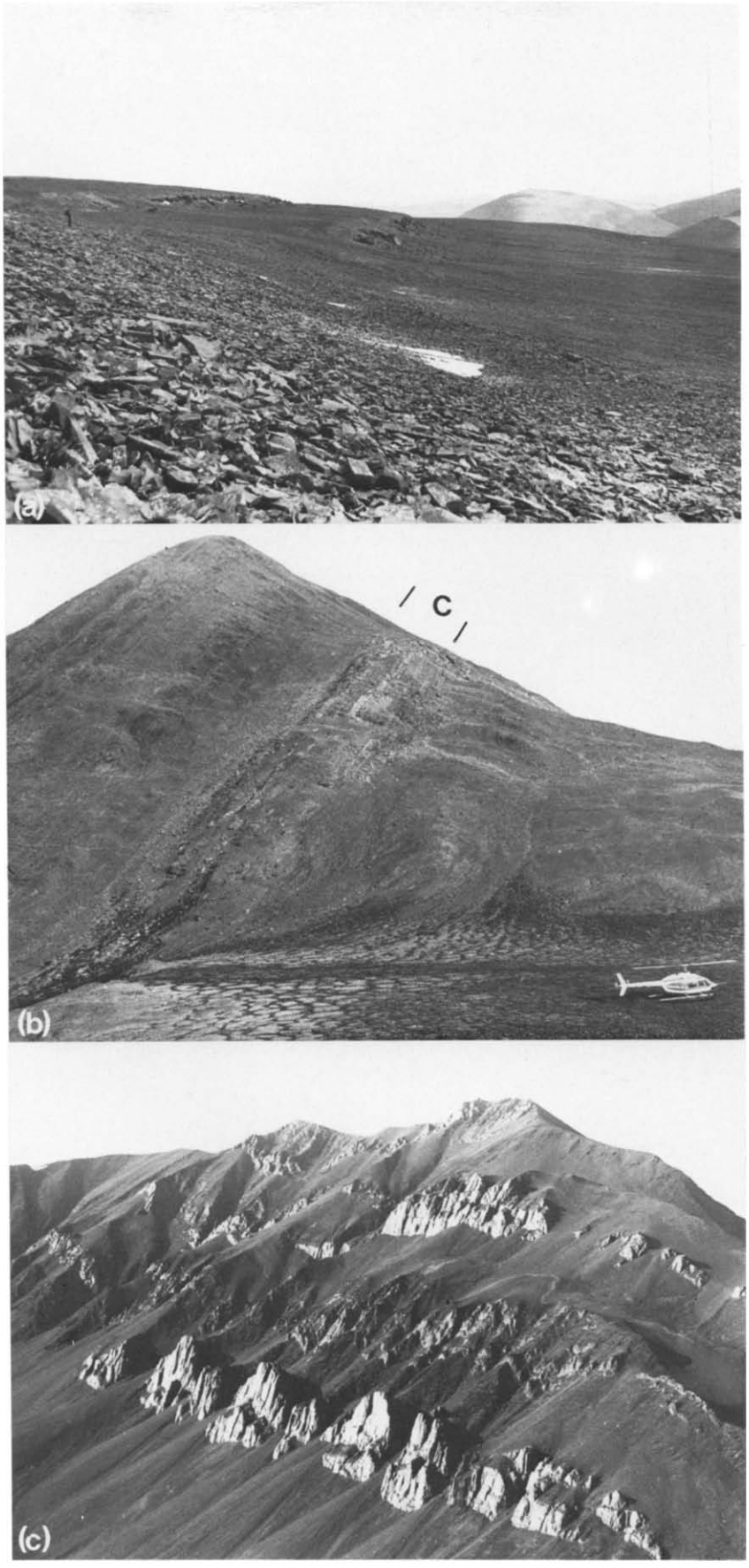

Fig. 7. (a) Silurian turbidites on the plateau in the southern part of the Nordkroneli area. The sandstone beds form terraces in the landscape, the orientation of which is very difficult to obtain in the field, but easily measured in the instrument. Person on the left side of the picture gives the scale. (b) Outcrop of easily measured conglomerate bed (C). The conglomerate overlies Ordovician turbidites and is overlain by ordivician cherty shales. (c) Steeply inclined Ordovician cherty shales. The wall-like exposures are excellent for measurement. Height of ridge is *c.* 500 m.

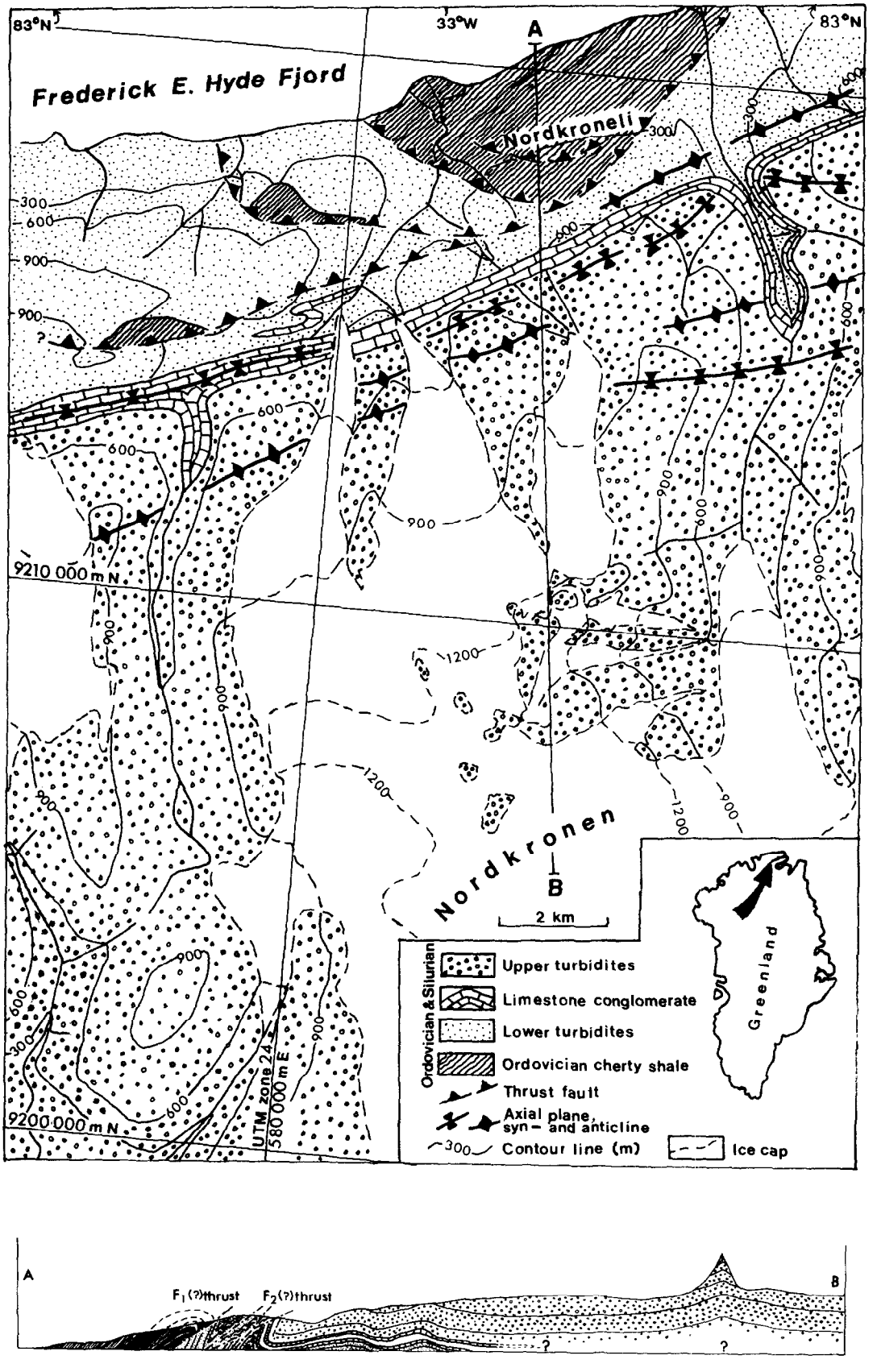

Fig. 6. Geological map of the area Nordkroneli, Peary Land, North Greenland.

the fold belt with unfolded strata in the southernmost part and increasing deformation towards the north.

The stereo model Nordkroneli

The stereo model covering the area of Nordkroneli (Figs. 4, 5 and 6) has been selected to illustrate the application of the method in a detailed study. The southern part of the ice-covered Frederick E. Hyde Fjord is seen in the northern part of the stereo model (Fig. 4). In the central part of the area an ice cap surrounds Nordkronen, one of the highest and most spectacular mountains in North Greenland. From the ice cap four glaciers flow towards the north, and a drainage pattern of consequent steams outlines the topography.

The greater part of the model area is built up of a sequence of Silurian turbidites more than 1 km thick. The typical pancake-shaped erosion pattern of the mountains in the unfolded part of the area can be seen in the southern half of the model. In the middle part of the model the turbidites are deformed into open folds, and in the north-eastern corner a large syncline overturned towards the south is outlined by a limestone-conglomerate unit on both sides of the stream. North of this syncline the rocks are intensely folded, and Lower Ordovician black shales and Upper Ordovician cherty shales have been thrust over the Silurian turbidites.

All the data recorded in the stereo model are plotted in the plot-map Fig. 5. The smallest plane measured for the structural investigation was 800 m^2. This gives an indication of the minimum size of the structures that can be examined in the 1:150,000 aerial photos. (The minimum size in 1:50,000 photos is *c.* 100 m^2). The average size of measured planes is however 2–3 times larger. The maximum size of measured planes was limited by the style of deformation. In the Nordkroneli area the most extensive plane measured was the axial plane of the syncline in the NE corner of the area (Fig. 5); this has an area of 185,000 m^2. Axial planes are relatively easy to measure where several hinge zones are exposed in an area of suitable relief, and the closure is not too rounded. The bedding planes applied in the fold axis calculations are less than half this size.

The planes measured were bedding planes separating different lithologies, which are seen as differences in grey tone and texture in the photos. Experience shows that as more time is spent looking at the aerial photos in the instrument, more details and variations can be recognized. This is especially the case for the uniform turbidites where the competent sandstone beds form terraces while the shales are eroded and scree-covered (Fig. 7a). Conglomerate beds with thicknesses in the range 3–20 m (Fig. 7b) have been found to provide very good measurable surfaces. In the fold belt area north of Frederick E. Hyde Fjord steeply inclined cherty shales form wall-like outcrops where the bedding planes are defined very precisely (Fig. 7c).

The values of the standard error of the fold axes calculated from photogrammetric data increase from S to N in the Nordkroneli area. In the southern part of the folded area all the fold axes have rather small standard errors. This is due to the fold style with upright folds and interlimb angles close to 90°. The fold axis C in Fig. 8 has a large error but has been accepted because the fold is inclined. Fold axes can be calculated with less confidence on overturned folds than in folds with flanks dipping in opposite directions.

The plot map (Fig. 5) presents the main features of the area. The main lithostratigraphic units are clearly seen on the aerial photos (Fig. 4); the difference between the two turbidite units (compare Fig. 4 and Fig. 6) is enhanced by their different tectonic behaviour. The plot also serves as a structural map and illustrates the increasing degree of deformation towards the north.

The geological map (Fig. 6) has been drawn on the basis of the plot map (Fig. 5) but in addition includes data obtained during 12 days of field work (Pedersen 1979). The field work confirmed the existence of the structures interpreted and measured in the stereo plotter. The lithological units were examined with emphasis on such

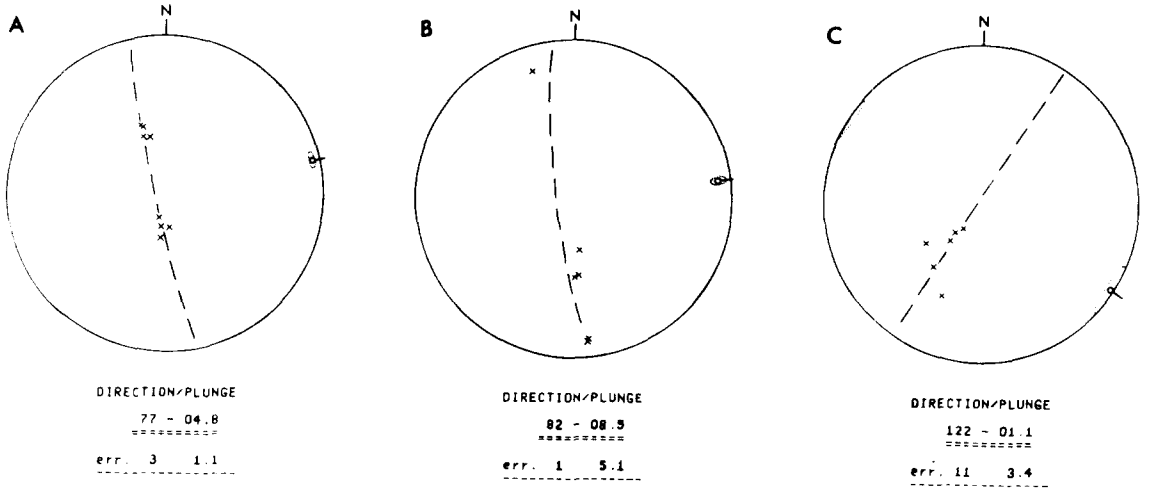

Fig. 8. Three stereograms showing the calculation of fold axes in the Nordkroneli area. The degree of deformation increases from A to C. A is an open upright fold, B is a close to tight fold overturned to the S, and C is a tight inclined fold with SW vergence. The dotted area around fold axis limits the standard error. Equal area projection, lower hemisphere.

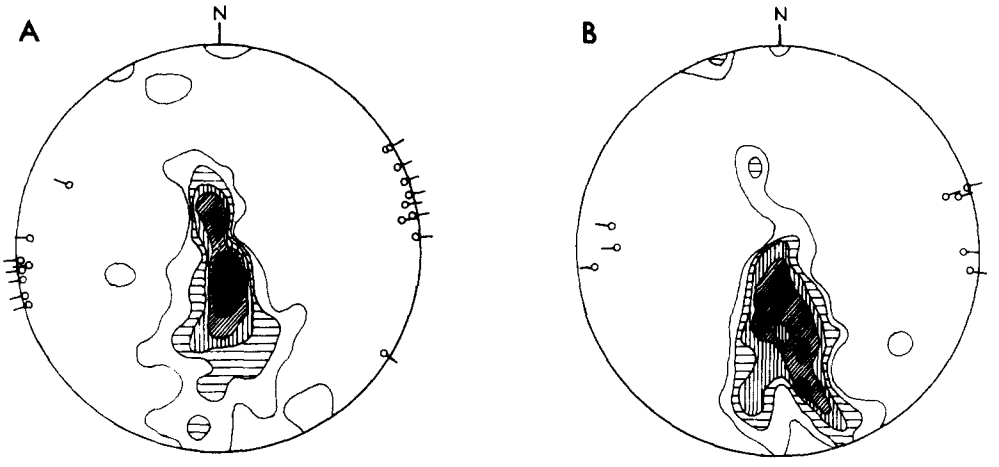

Fig. 9. Comparison of photogrammetrically obtained measurements and field measurements in the Nordkroneli area. Poles to bedding are contoured. Equal area projection, lower hemisphere. (a) Photogrammetrically obtained measurements. Contour intervals 1,2.5, 5,7.5, 10 and 15%; number of planes = 120. Besides the strong E–W to ENE–WSW trend there are two deviating NW–SE fold axes. (b) Field measurements. Contour intervals 1,2.5, 5,7.5, 10 and 12.5%; number of measurements = 79. Fold axes measured directly on folds in the field.

features as composition, sedimentary structures, fossils, small-scale folds and thrust, which cannot be studied photogeologically. Accordingly, parts of the photogeological interpretation had to be revised, especially in the northern part of the area. For instance it was first realised through the discovery of Lower Ordovician graptolites that the black cherty shale unit to the north was thrust over the Silurian turbidites. After the field season the stereo model was re-examined and the final geological map could be drawn (Fig. 6).

In Fig. 9 a comparison is presented between photogrammetrically obtained measurements and field measurements from this area. The stereograms in Fig. 9 show a marked axis trend E–W to WSW–ENE. This is the general trend of the North Greenalnd Fold Belt in Peary Land (Dawes 1971, Dawes & Soper 1979, Pedersen 1979). The most impressive fold belonging to this phase of deformation is the southwards-overturned synclinal structure outlined by the limestone-conglomerate unit in the north-eastern part of the area. South of this syncline the fold deformation gradually fades out. North of the syncline the beds are overturned to the south which results in a remarkable change in the outcrop pattern.

In the stereogram Fig. 9(a) two fold axes show a NW–SE trend which deviates markedly from the general E–W trend (Fig. 9a and b). A closer look at one of these folds, that with axis 122°/1°, and the fold 82°/9° (Figs. 8b and c) both situated in the NW corner of the area, suggests an explanation for this. The fold axis 122°/1° is situated above and NE of the fold axis 82°/9°. Both flanks of the 122°/1° fold dip towards NE. The 82°/9° fold axis belongs to the general E–W trending fold deformation, but its plunge deviates to the ENE. This could lead to the conclusion that a deformation leading to axes trending NW–SE tilted the beds before the folding with axes trending E–W. This is in agreement with the refolded thrust fault deformation described from the opposite side of Frederick E. Hyde Fjord.

The structural mapping of the Frederick E. Hyde Fjord region

The E–W trending fold structures were described by Dawes (1971, 1976) and Dawes & Soper (1973, 1979). However a trend variation in the Frederick E. Hyde Fjord region was recorded by Haller (1971) in a structural map of the fold belt based on interpretation of aerial photos. In the summer of 1978 the present author visited this region and westwards-directed thrust faults were observed (Pedersen 1979). In the six months following the field season 32 vertical aerial photos at scale 1:150,000 (sea level) and additional detailed photos at scale 1:54,000 were examined in an attempt to assess the extent of this thrust fault deformation and the nature of the abnormal trend variation. All possible bedding planes were measured and fold axis calculations carried out. In Fig. 10 a representative number of measured strike-and-dips and calculated fold axes have been plotted in a compiled plot-map. The strike-and-dip symbols show up the characteristic curved structural pattern, which deviates remarkably from the general E–W trend of the fold belt.

The photogrammetric work as it progressed indicated that thrust fault deformation had affected the whole area shown in Figs. 10 and 11, but subsequent recording of steeply plunging fold axes indicated an additional phase of deformation. Thus a hypothesis of refolded thrust faulting and folding was developed. This could not, however, be proved on the aerial photos alone, which only revealed complex structural relationships. Fortunately it was possible to visit the area in 1979 and test the hypothesis in the field.

Before the 1979 field season a new map of the Frederick E. Hyde Fjord region at scale 1:100,000 was produced. In addition, 3000 km^2 were drawn up on 1:50,000 maps with contour interval 100 m, and all major structural features were plotted. These plots served as base maps for the structural field investigations. During the field season the

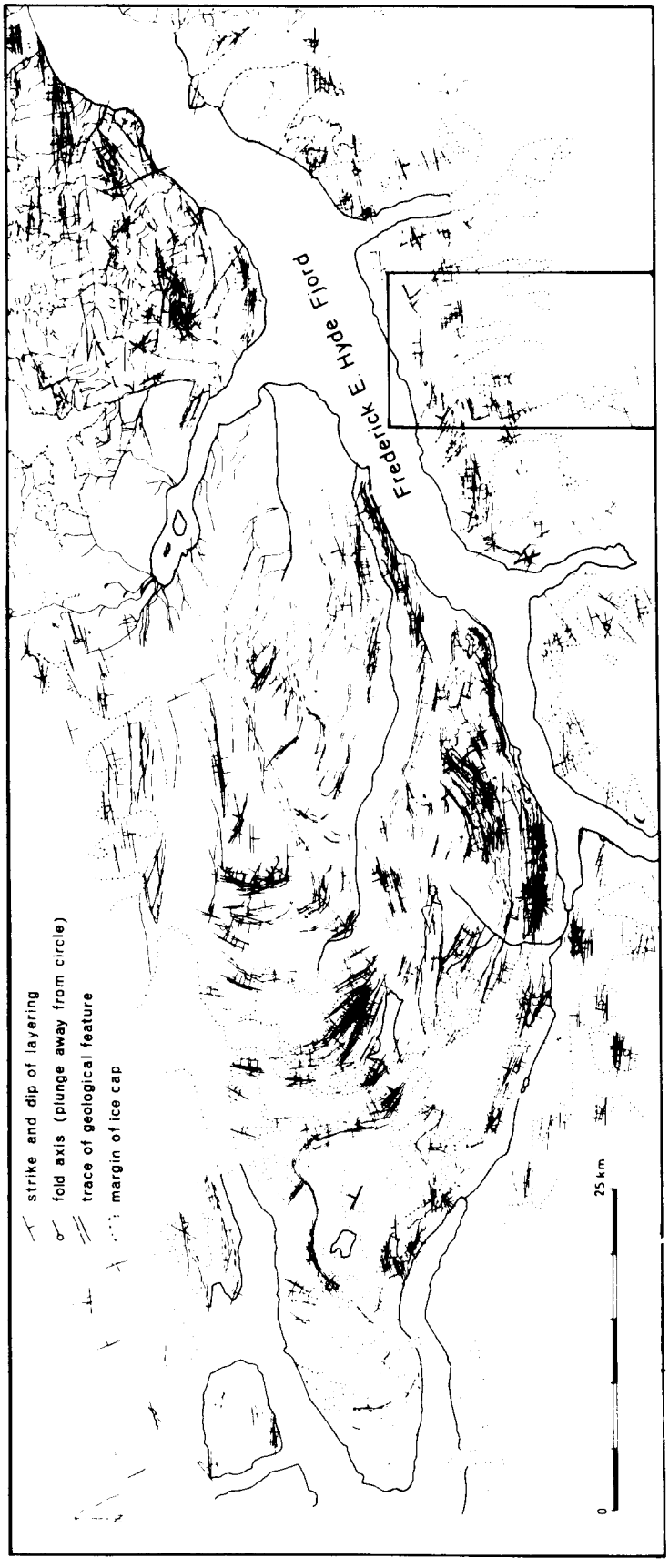

Fig. 10. Computer calculated and Calcomp plot map of the structures recorded in the Frederick E. Hyde Fjord Region. The Nordkroneli area is framed just below Frederick E. Hyde Fjord.

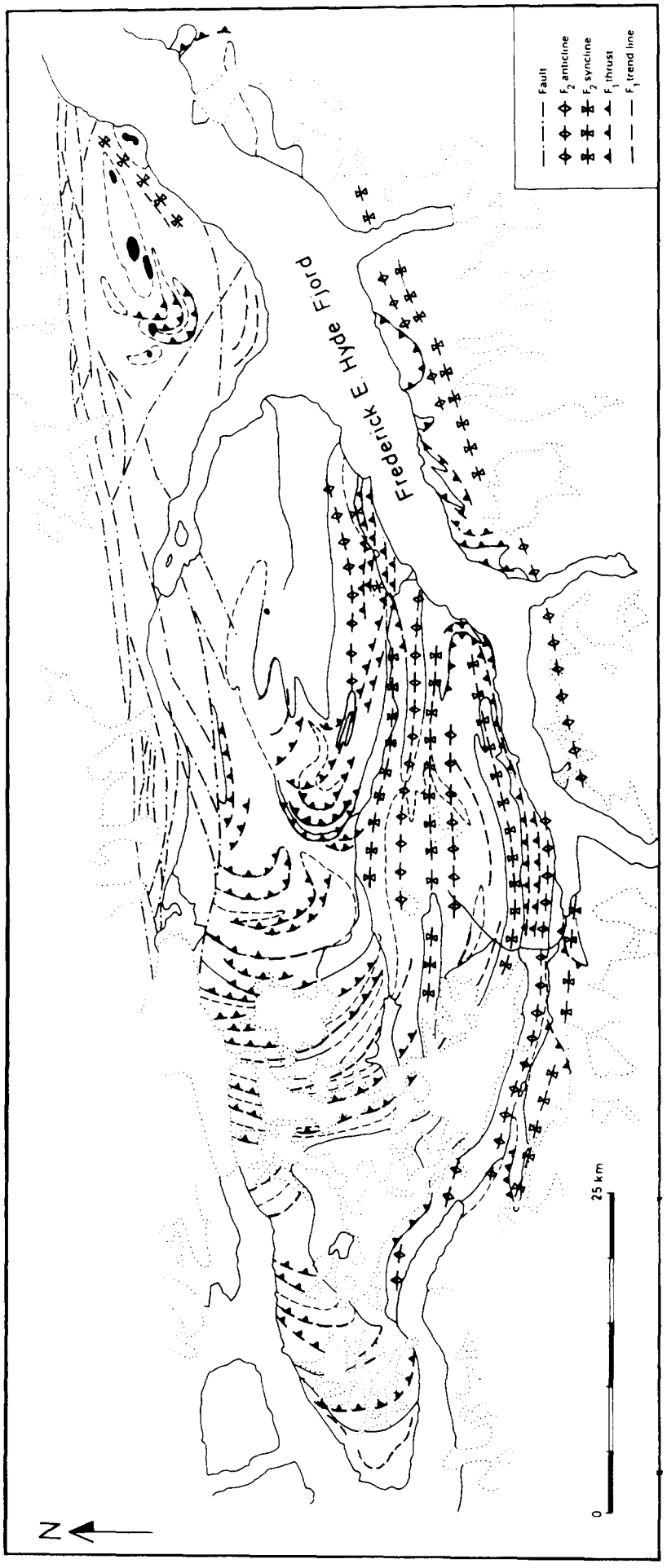

Fig. 11. Structural map of the Frederick E. Hyde Fjord Region. The E–W trending fault zone in the northern part of the map is the Harder Fjord fault, a regional fault zone across which the thrust fault deformation cannot be traced. Black areas in the eastern part of the map are intrusive centres with gabbro and serpentinite.

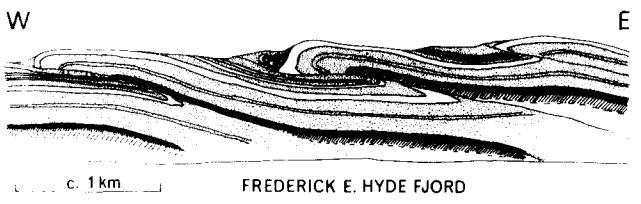

Fig. 12. Thrust fault structures exposed in a cliff section on the north side of Frederick E. Hyde Fjord. White bands are conglomerate beds, the stippled unit is turbidites and the black band is black cherty shales. The cliff section is approximately perpendicular to fold axes of the anti clines.

hypothesis was checked and received support from field observations, and it has now been shown that the curved trend lines result from interference between a first phase of deformation, which resulted in thrust faulting, and a second phase which caused folding about E–W axes (Pedersen 1980) (Fig. 11).

Thrust fault deformation affects about 200–400 m of Cambrian (?) mudstones overlain by about 1000 m of Ordovician cherty shales, turbidites and conglomerates. The stratigraphic sequences may be repeated up to four times in one cliff (Fig. 12) and the horizontal displacement on the thrusts has been estimated to range from 1 to 10 km. The thickness of the thrust sheets varies from 100 to 300 m, and the mudstones served as zones of décollement. Competent conglomerate units in the turbidites form forelimb anticlines and backlimb synclines in the thrust sheets (Fig. 12).

In the second phase of deformation open upright folds were formed with amplitudes of 500 m and wave-lengths of 2–3 km. At the southern margin of the fold belt these folds are overturned to the south, while in the north western part of the area studied the folds become slightly overturned to the north.

In the regional structural framework the second phase of deformation is responsible for the major bending of the thrust fault structures which form the curved trend lines seen on Figs. 10 and 11.

CONCLUSION

Computer supported photogrammetry can be applied successfully in the study of geological structures. The method may be used advantageously in the mapping of large inaccessible areas with sparse vegetation, such as high-Arctic North Greenland. Other physiographical regions where the method could be recommended are deserts, desert highlands and steep mountainous areas. Furthermore the photogrammetric method is a powerful tool in the study of large tectonic structures as these can be seen and measured in one stereo model while they are often difficult to appreciate in the field.

The structural elements are calculated from photogrammetrically measured planes which are an order of magnitude larger than planes measured by the geologist in the field.

The work on the stereo plotter results in a map of lithological units, measurements of strike and dip as well as calculated fold axes, and constitutes the basis for an interpretation resulting in a geological map.

In the present study it has been found that open to close folds may be safely interpreted photogrammetrically, while the interpretation of intensely folded areas requires checking in the field.

The photogrammetric method described has been invaluable in the attempt to unravel the complex geology of the Frederick E. Hyde Fjord region in the limited time available.

Acknowledgements—H. Jepsen and K. Dueholm are thanked for numerous discussions during the progress of the work. O. Winding assisted as photogrammetric operator. N. Henrixsen and T. C. R. Pulvertaft kindly read an earlier version of the paper and offered many helpful suggestions and T. C. R. Pulvertaft improved the English text. The paper is published by permission of the Director of GGU. The paper was completed while the author held a grant from the University of Copenhagen which is gratefully acknowledged.

REFERENCES

Dawes, P. R. 1971. The North Greenland fold belt and environs. *Bull. geol. Soc. Denmark* **20,** 197–239.

Dawes, P. R. 1976. Precambrian to Tertiary of northern Greenland. In: *Geology of Greenland.* (edited by Escher, A. & Watt, W. S.) Geol. Surv. Greenland, Copenhagen, 248–303.

Dawes, P. R. 1977. Geological photo-interpretation of Hall Land: part of the regional topographical geological mapping of northern Greenland. *Rapp. Grønlands geol. Unders.* **85,** 25–30.

Dawes, P. R. & Soper, N. J. 1973. Pre-Quaternary history of North Greenland. In: *Arctic Geology.* (edited by Pitcher, M. G.) *Mem. Am. Ass. Petrol. Geol.* **19,** 117–134.

Dawes, P. R. & Soper, N. J. 1979. Structural and stratigraphic framework of the North Greenland fold belt in Johannes V. Jensen Land, Peary Land. *Rapp. Grønlands geol. Unders.* **93,** pp. 40.

Dueholm, K. S. 1976. New instruments for geological photo-interpretation and mapping. *Rapp. Grønlands geol. Unders.* **80,** 144–148.

Dueholm, K. S. 1979. Geological and topographic mapping from aerial photographs. In: *Geological and Topographic Mapping from Aerial Photographs.* (edited by Dueholm, K. S.) Institute of Surveying and Photogrammetry, DTH, Denmark, 9–142.

Dueholm, K. S. 1980. Computer supported geological photo-interpretation. *Proc. 14th Congr. Int. Soc. Photogrammetry.* Hamburg, West Germany, 1–10.

Dueholm, K. S., Pedersen, A. K. & Ulff-Møller, F. 1977. High precision photogrammetric methods in geological mapping. *Rapp. Grønlands geol. Unders.* **81,** 53–56.

Haller, J. 1971. *Geology of East Greenland Caledonides.* London, Interscience.

Jepsen, H. F. & Dueholm, K. S. 1978. Computer supported geological photo-interpretation. *Rapp. Grønlands geol. Unders.* **90,** 146–150.

Lattman, L. H. & Ray, R. G. 1965. *Aerial Photographs in Field Geology.* Holt, Rinehart & Winston, Inc., New York.

Miller, V. C. 1961. *Photogeology.* McGraw-Hill, New York.

Pedersen, S. A. S. 1979. Structural geology of Central Peary Land, North Greenland. *Rapp. Grønlands geol. Unders.* **88,** 55–62.

Pedersen, S. A. S. 1980. Regional geology and thrust fault tectonics in the southern part of the North Greenland fold belt, North Peary Land. *Rapp. Grønlands geol. Unders.* **99,** 79–87.

Surlyk, F., Hurst, J. M. & Bjerreskov, M. 1980. First age-diagnostic fossils from the central part of the North Greenland fold belt. *Nature, Lond.* **286,** 800–803.

Wolf, P. R. 1974. *Elements of Photogrammetry.* McGraw-Hill, New York.